https://doi.org/10.37375/bsj.v7i20.3640

A Multidisciplinary Risk Assessment of Pressure Vessel Integrity and Hazardous Area Classification in n-Heptane Handling Operations

*Essa Shawail Faraj Zaid Magdi Buaisha

تاريخ الاستلام: 7 / 8 / 2025 اجازة النشر: 6/10/ 2025 تاريخ النشر: 17/ 11/ 2025

Abstract: This multidisciplinary study assesses risks in a high-pressure vessel storing flammable n-heptane. Using failure diagrams, corrosion modeling, and hazard zoning, it provides a holistic safety evaluation. Results show structural integrity is highly pressure-sensitive, with 60 MPa causing near-critical stress versus safe operation at 30 MPa. Corrosion modeling predicted a 0.92 mm wall loss over 20 years, remaining within safety limits. Vapor dispersion ranged from 2.99–13.86 m, informing electrical and ventilation designs. The research underscores integrating engineering disciplines for predictive safety strategies and promotes inherent safety over add-on measures.

Keywords: Pressure Vessel, Fracture Mechanics, Corrosion Rate, n-Heptane, Inherent Safety

تقييم المخاطر المتعلقة بسلامة أوعية الضغط وتصنيف المناطق الخطرة في عمليات مناولة ال ن–هبتان

عيسى شوايل: قسم الهندسة الكيميائية، كلية الهندسة، جامعة سرت، **ليبيا**

فرج زيد: قسم الهندسة الكيميائية، كلية الهندسة، جامعة سرت، ليبيا

مجدي بوعيشة: الإدارة العامة للتفتيش والقياس – المؤسسة الوطنية للنفط، طرابلس، ليبيا

المستخلص: يقيّم هذا البحث متعدد التخصصات المخاطر في الاوعية عالية الضغط العاملة بـ" ن–هبتان . "أظهر التحليل الميكانيكي أن ضغط 60 ميجاباسكال يُولّد إجهادات حرجة، بينما يظل ضغط 30 ميجاباسكال آمنًا .وتوقعت نمذجة التآكل فقدانًا بسمك 0.92 مم خلال 20 عامًا مع الحفاظ على معاملات السلامة .كما قدّر تحليل المخاطر تشتت البخار بين 2.99 و 13.86م .3تؤكد النتائج على أهمية تطوير ودمج التخصصات الهندسية و استراتيجيات السلامة التنبؤية المتكاملة لتعزيز السلامة الكامنة في التصميم.

الكلمات المفتاحية: أوعية الضغط، ميكانيكا الكسر، معدل التآكل، ن–هبتان، السلامة المتأصلة

Introduction:

Pressure vessels play a critical role in several industries, including oil refining, gas production, nuclear energy, chemical processing, thermoelectric power generation, and alcohol manufacturing. These vessels are designed to safely contain substances at high pressures and sometimes extreme temperatures. Because of their function, pressure vessels are governed by strict engineering codes and safety standards such as ASME section VIII and BS 7910 (American Society of Mechanical Engineers [ASME], 2010; Andrews et al., 2018; British Standards Institution, 2019). Failure of a pressure vessel can have catastrophic consequences, including explosions, toxic leaks, and structural damage, which may lead to

* **Department of Chemical Engineering, Faculty of Engineering, University of Sirte, Libya: Corresponding author Email. essa.shawail@su.edu.ly**

Department of Chemical Engineering, Faculty of Engineering, University of Sirte, Libya: faraj.zaid@su.edu.ly

The General Directorate of Inspection and Measurement- National Oil Corporation (NOC), Tripoli, Libya. mdawood@noc.ly

injury, death, or severe environmental impact. The evaluation of structural integrity seeks to prevent possible failures by meticulously assessing structural damage using detailed inspection techniques and analytical methods. These approaches are essential for extending the safe operational lifespan of the facility and improving the durability of its components (Medina, 2014).

Two of the most prevalent failure mechanisms in pressure vessels are fracture and corrosion (Ayyub et al., 2015; Fontana, 1986; Tantichattanont et al., 2007). Fractures typically initiate from pre-existing manufacturing defects, fatigue loading, or residual stresses, and may propagate under cyclic or sustained stress conditions. If unchecked, they can grow rapidly, culminating in brittle or ductile rupture. Corrosion, by contrast, is a gradual but insidious mechanism that can reduce the wall thickness of the vessel over time. This reduction undermines the vessel's ability to contain pressure, increasing stress on remaining material and thereby amplifying the risk of crack growth or buckling. Recent studies have also shown that sulfur containing organic inhibitors, such as methyl carbazodithoate, can significantly reduce corrosion in acidic environments, suggesting a viable pathway for enhancing vessel longevity under aggressive chemical conditions (Mohammed et al., 2019).

Expanding on this, a wide range of heterocyclic compounds---particularly those containing nitrogen and sulfur atoms---have demonstrated high inhibition efficiencies due to their ability to chelate with metal ions and create stable films that prevent corrosive species from attacking the metal substrate. For instance, research involving carbon steel in acidic CO_2 and H_2SO_4 environments has revealed inhibition efficiencies exceeding 80% when these organic inhibitors are combined with halide ions, underscoring the synergistic role of molecular additives (Bentiss et al., 2012). In more aggressive applications, such as acid stimulation in oilfields, formulations blending Mannich base derivatives with metal salts have proven effective even under high-temperature conditions, achieving inhibition rates above 95% at temperatures up to 180 °C (Quraishi et al., 2014).

Alongside chemical protection, the structural assessment of vessels is equally critical. Recent advances in multi-physics modeling such as phase-field simulations now offer improved predictive capability by explicitly simulating corrosion-fatigue interactions, intergranular attack, and the evolution of corrosion fronts in polycrystalline steels (Martínez-Pañeda, 2024). In parallel, microstructure-sensitive electro-chemo-mechanical phase-field models have recently been developed to capture the effects of grain orientation and double-layer charging dynamics on pit initiation and crack morphology under stress (Makuch et al., 2024). Moreover, a mesoscale phase-field model published in mid-2025 simulates intergranular corrosion in ferritic/martensitic steels exposed to liquid metal environments, emphasizing the critical role of grain boundary chromium depletion in accelerating corrosion (Lhoest et al., 2025).

Turning to empirical inhibition studies, novel organic compounds have continued to yield high efficiencies well beyond 2023: for example, tetraphenylethylene-based thiocyanate inhibitors achieved over 97% inhibition of carbon steel in 0.5 M H_2SO_4 (Chen et al., 2023). Similarly, dextran-based polymeric inhibitors have demonstrated effective, eco-friendly protection of carbon steel in circulating cooling water systems, expanding the scope of inhibitor application beyond simple acidic media (Xu & Chen, 2024). Moreover, recent numerical studies have highlighted how pitting corrosion significantly reduces fatigue life in

clinched joints under cyclic stress, a scenario highly relevant to welded pressure vessel components under pressure fluctuation (Recent Numerical Studies, 2025).

This study investigates a pressure vessel that stores n-heptane, a hydrocarbon that poses dual threats: mechanical (due to high pressure) and chemical (due to flammability). N-heptane's low flash point and high vapor pressure make it especially dangerous in the event of leakage. Therefore, in addition to structural and corrosion analyses, a robust hazardous area classification is necessary to ensure safe design and operation.

To address these complexities, a comprehensive multidisciplinary approach was adopted, encompassing the following methodologies: A fracture mechanics analysis was performed utilizing the Failure Assessment Diagram (FAD) to assess the behavior of cracks under operational stresses (ASME, 2010). An electrochemical corrosion model was developed, drawing on polarization resistance and Tafel slope data to estimate the material degradation over time (Buchanan & Stansbury, 2005). A hazardous area classification was conducted through dispersion modeling to ascertain the spatial extent of explosive vapor clouds around potential leak sites.

By integrating these three approaches, the study offers a risk-informed framework that enhances safety, optimizes maintenance, and supports compliant and efficient design. It also supports the application of inherent safety strategies that aim to eliminate hazards rather than merely control them.

Methodology:

To comprehensively assess the safety and performance of the pressure vessel, a three-pronged methodology was utilized, incorporating mechanical fracture analysis, electrochemical corrosion modeling, and hazardous area zoning. This approach effectively addresses all aspects of risk, including structural, temporal, and environmental considerations.

Fracture Mechanics Assessment:

To assess the structural vulnerability of the pressure vessel, a semi-elliptical surface crack was hypothesized in the cylindrical wall. The stress analysis encompassed calculations for both hoop and axial stresses, with the stress intensity factor (K_I) determined through recognized equations from the field of fracture mechanics (American Petroleum Institute, 2016; Anderson, 2017; Yagawa et al., 1985):

$$K_I = y\sigma\sqrt{\pi a} \quad (1)$$

The stress intensity factor geometry term (y) is given by

$$Y = \frac{1.12}{\sqrt{1+1.464(a/c)^{1.65}}} \quad (2)$$

The internal collapse pressure (Pc) is given by

$$Pc = \sigma_y \left[\frac{a}{} + \left(\frac{Ri}{}\right)\ln\left(\frac{Ro}{}\right)\right] \quad (3)$$

Where:

$$M = \sqrt{\left(1+\frac{1.61C^2}{Ria}\right)} \quad (4)$$

$$\text{Axial stress } \sigma_a = \frac{\text{Pr}}{2t} \quad (5)$$

$$\text{Hoop stress } \sigma_h = \frac{\text{Pr}}{t} \quad (6)$$

The fracture toughness

$$\text{Kr} = \frac{K_{Iapplied}}{K_{IC}} = \frac{y\sigma\sqrt{\pi a}}{K_{IC}} \quad (7)$$

The load ratio

$$\text{L}_R = \frac{P_{appliedload}}{P_{CCollapsebad}} \quad (8)$$

The safety factors

$$\text{F}^L = \frac{OB}{OA} \quad (9)$$

These allowed assessments of failure potential under varying pressure conditions. The Failure Assessment Diagram is shown in (Figure 1).

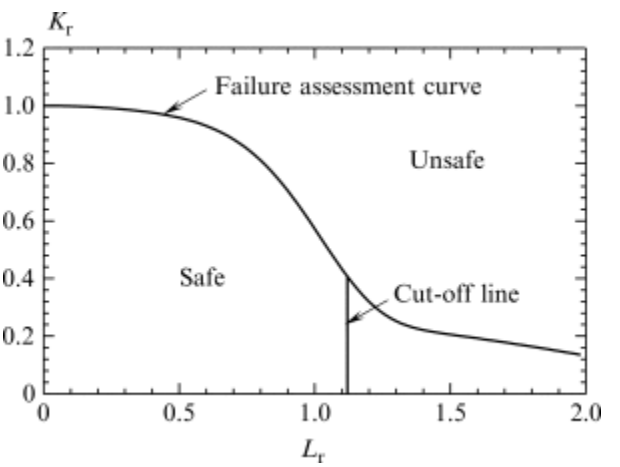

Figure 1: Failure Assessment Diagram. [Qian, X. (2016)].

Corrosion Modeling:

Corrosion rate was evaluated through electrochemical testing, using polarization curves and the Tafel extrapolation method to calculate the corrosion current density (I_{corr}) (Bard et al., 2022; Buchanan & Stansbury, 2005; Fontana, 1986).

The formula used was:

$$\text{I}_{corr} = \frac{\beta a x \beta c}{2.3x(\beta a + \beta c)xR_p} \quad (10)$$

Where:

- β_a, β_c = anodic and cathodic Tafel slopes (V/decade)
- R_p = polarization resistance ($\Omega \cdot cm^2$)

The operating stresses are given by using the following equation:

$$\sigma_h = \frac{pd}{2t} \quad (11)$$

Where:

p = Internal pressure

d = Internal diameter

t = Wall thickness of the cylinder

Hazardous Area Classification

Hazardous area classification assessed the potential for flammable vapor accumulation in the event of leaks. The release rate (*G*) and volume flow rate (*Q*) were calculated as (American Petroleum Institute, 2016; Energy Institute, 2015; International Electrotechnical Commission, 2020):

$$G = 0.00586 \times A \times P1 \times (M/T1)^{0.5} \quad (12).$$

Where:

A = Cross section of leak path in m^2

P1= Absolute pressure upstream of release in pa

M= Molecular weight

T1= Absolute temperature upstream of release in k

Volume flow rate (Q) is given by

$$Q = 0.0821 \times (G \times T1/M) \quad (13).$$

Release from high level point source is given by

$$X = (920 \times Q/E)^{0.55} \quad (14).$$

Release from ground level point source is given by

$$X = (1840 \times Q/E)^{0.55} \quad (15)$$

Where:

E = Lower explosive limit in % Vol

Depending on leak orientation (horizontal/vertical), the constant *E* was adjusted.

Results and Analysis

Fracture Mechanics Evaluation

Table 1: Parameters established for the operational pressure vessel

Given parameters	Vessel diameter(m)	Vessel radius (m)	Vessel external radius (m)	Vessel wall thickness (t)	crack of depth (a)	Yield stress σ_y	Tensile strength σ_u	Fracture toughness K_{IC}
	2m	1m	1.1m	100mm	0.03m	750MPa	900MPa	170MPa $\sqrt{m}$

Two pressure scenarios 60 MPa and 30 MPa were evaluated to understand the vessel's response to internal pressure with an existing surface crack:

A Semi-circular pressure vessel is suggested thus; a = c = 0.03m

Using the equations from Section 2.1, the load ratio Lr, the fracture toughness Kr and safety factors were calculated in Table 2 as follows:

Table 2: The results for Kr, Lr, and safety factors obtained at pressures of 60 and 30 MPa.

								At 60 MPa:
M	Pc	$L_R = \frac{P_{appliedload}}{P_{CCollapsebad}}$	Y	σ_u	σ_a	K_I	$Kr = \frac{K_{Iapplied}}{K_{IC}}$	F^L
1.02386	69.85×10^6 MPa	0.86	0.7135	600MPa	300MPa	131.39MPa	0.77	0.99
								At 30 MPa:
M	Pc	$L_R = \frac{P_{appliedload}}{P_{CCollapsebad}}$	Y	σ_u	σ_a	K_I	$Kr = \frac{K_{Iapplied}}{K_{IC}}$	F^L
1.02386	69.85×10^6 MPa	0.43	0.7135	300MPa	150MPa	65.69MPa	0.39	2

As can be seen in the results at 60 MPa, the fracture toughness (Kr = 0.77) and the load ratio (LR = 0.86). These values placed the integrity of the vessel outside the allowable limits specified in the Failure Assessment Diagram (Figure 2). The intersection of the Kr and LR values with the FAD curve indicated imminent failure risk under this loading. Any increase in pressure or further crack propagation would likely result in catastrophic failure. However, at 30 MPa, Kr = 0.39 and LR = 0.43. This point was comfortably situated within the established safe zone of the FAD, indicating a significant margin of structural integrity. The vessel can safely operate at 30 MPa even with existing flaws. The vessel is structurally unsafe at 60 MPa and safe at 30 MPa, assuming no change in crack size or shape. Figure 2 also illustrates that when the working internal pressure of the vessel is set at 30 MPa, the safety factor (F^L) remains high. However, at a working internal pressure of 60 MPa, the safety factor decreases significantly, indicating potential risks. Therefore, operating the vessel at this elevated pressure is not advisable, as it poses a danger to its integrity. It is crucial to ensure that the pressure does not exceed 30 MPa in order to prevent reaching the critical threshold of 60 MPa, which could result in damage to the vessel.

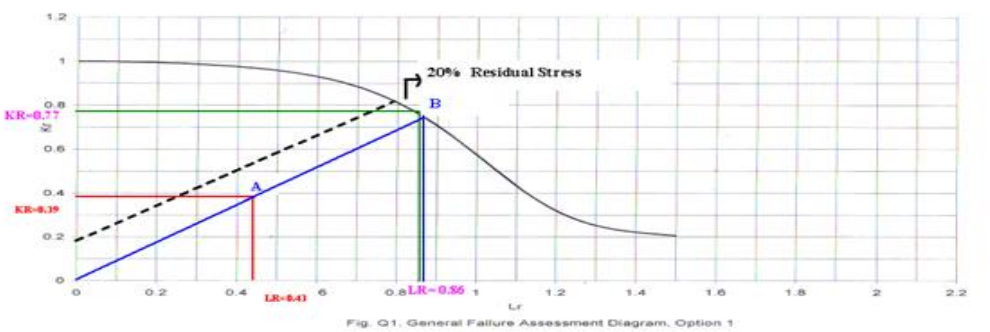

Figure 2: Illustrates Failure Assessment Diagram (Kr vs Lr)

Corrosion Impact Assessment

Table 3: Specifications defined for the pressure vessel

Given parameters	operating pressure (P)	yield strength σ_u	Length	Diameter (d)	Wall thickness (t)	Thickness loss µA/cm^2	Tafel slopes mV/decade	
	7MPa	500MPa	250 mm	75 mm	2.5 mm	0.0116 mm/y	βa = 60	βc = 120

Utilizing the provided data and the equations outlined in Section 2.2, the corrosion rate (I_{corr}), the final operating stress, and thickness loss over time were determined in the Summary below:

Summary of Findings

Parameter	Initial Value	After 20 Years	Critical Limit
Thickness	2.5 mm	1.58 mm	0.525 mm (unsafe)
Hoop Stress	105 MPa	166 MPa	500 MPa (yield)
Safety Factor	~4.76	3.0	1.0 (failure)

The polarization graph was plotted, facilitating the calculation of R_p = 0.0005 (mA/cm²/mV) based on the linear relationship depicted in (Figure 3). The corrosion rate of the vessel's material is measured at 8.69 (µA/cm²). Based on standard corrosion data, a corrosion rate of 1 µA/cm² leads to an annual thickness loss of 0.0116 mm/year. Applying this conversion, the vessel's corrosion rate translates to an annual thickness loss of 0.1 mm/ year when operating continuously. Over a 20-year operational lifespan, continuous exposure would result in a total thickness loss of 2.0 mm. However, the vessel only operates 4000 hours per year (not full-time). To account for this, the effective corrosion time is calculated as: (4000/8760 ≈ 0.4578)

This means that the actual thickness loss over 20 years is about 0.92 mm rather than the full 2.0 mm. Initially, the vessel's wall thickness is 2.5 mm. After accounting for the adjusted corrosion loss, the remaining thickness after 20 years is 1.58 mm. This means the vessel's wall will gradually thin from 2.5 mm to 1.58 mm over two decades of operation. This calculation confirms that the vessel retains sufficient structural integrity after 20 years, as the remaining thickness is still well above the critical failure threshold.

The operating stress бi and final operating stress $б_f$ were found to be 105MPa and 166MPa.

The analysis of operating stresses indicates that, when compared to the material's yield strength of 500 MPa, the vessel will remain safe after 20 years of operation, as the stress levels are projected to reach only approximately 166 MPa. To assess the vessel’s ability to withstand these operating stresses, we can calculate the safety factor as follows:

Safety Factor = Yield Strength / Operating Stress

Safety Factor = 500 MPa / 166 MPa = 3

This calculation reveals a sufficiently high safety factor, suggesting that the vessel can continue to operate safely and does not require decommissioning after 20 years. To

determine the critical thickness at which the vessel would become unsafe for use, the following formula can be applied:

t = (7x75)/(2x500) = 0.525 mm

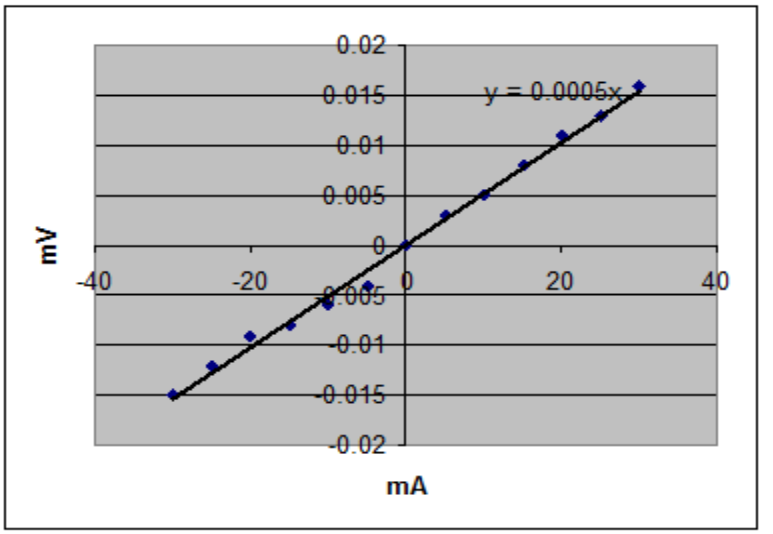

Figure 3: Polarization Curve

Hazardous Area Analysis

Using the equations from Section 2.3, dispersion distances were calculated for key component as the following:

Component	Area (m^2)	Mass Flow (kg/s)	Dispersion Distance (m)
Flange (1)	0.0001923	0.0654	3.87
Sample Point	0.0000706	0.2404	7.90
Pump	0.00196	0.667	13.86
Tanker Flange	0.00017	0.0579	3.68
Tank Overflow	—	—	7.26

The classification based on dispersion (Figure 4):

- Zone 0: Continuous presence of flammable vapor, including inside the tank and inside sealed pump enclosures
- Zone 1: Occasional presence under normal operation. Up to 4 m around sample ports, valves
- Zone 2: Vapor present only under abnormal conditions. Beyond 4 m for pump discharge, up to 14 m in extreme cases

These zones mandate explosion-proof equipment, ventilation, and zoning-compliant electrical layouts. The large dispersion distances emphasize the flammable risk of n-heptane and the importance of effective zoning. The different type of hazardous zones is shown in the figure below,

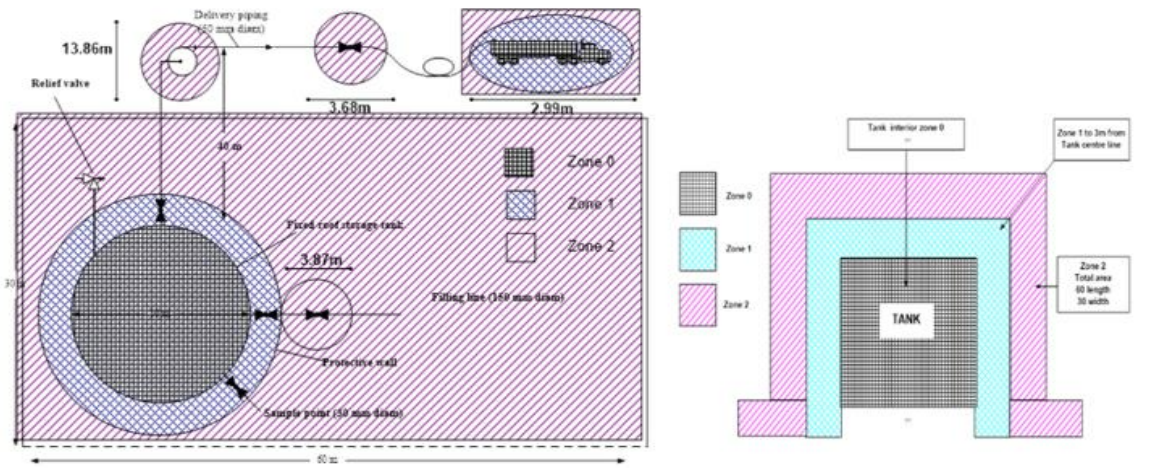

Figure 4: Shows the different type of hazardous zones

Discussion

The integrated results from fracture analysis, corrosion modeling, and hazardous area classification reveal several critical insights about the long-term safety and operability of the pressure vessel in n-heptane service.

Structural Integrity and Pressure Limits

The evaluation of fracture mechanics illustrates the intricate relationship between internal pressure and flaw tolerance. At an internal pressure of 60 MPa, the vessel nears the structural failure threshold, especially when minor crack geometries are present. The computed values of Kr = 0.77 and LR = 0.86 are positioned outside the safety zone of the Failure Assessment Diagram. This positioning signals that the vessel is at high risk of crack propagation or plastic failure (Figure 2). Moreover, an approximate increase of 20% in the residual yield stress would reduce the Kr value to 0.19, indicating that the vessel's structural integrity falls short of the acceptable limits defined by the Failure Assessment Diagram. Consequently, operating under these conditions is not advisable unless repairs or pressure reductions are made promptly. In contrast, when the vessel operates at 30 MPa, it demonstrates a significant safety margin, even when considering potential long-term corrosion effects (Figure 2). This disparity underscores the critical need for conservative design practices, routine inspections, and stringent operational protocols. In reality, numerous older vessels continue to function despite having unknown or undocumented flaws; thus, these findings advocate for the implementation of regular fitness-for-service (FFS) assessments as a standard practice in operations.

Figure 2 also illustrates that when the vessel operates at an internal pressure of 30 MPa, the safety factor remains sufficiently high. However, at a working internal pressure of 60 MPa, the safety factor diminishes significantly, indicating that operation at this pressure poses a significant risk to the vessel's integrity. Therefore, it is crucial to avoid exceeding the 30 MPa threshold to ensure the vessel's safety, as surpassing this limit could result in potential damage.

Corrosion Behavior and Lifecycle Safety

Although corrosion typically progresses more slowly than mechanical failure, its impact over long periods can be just as consequential. The estimated wall loss of 0.92 mm over 20 years may not appear severe, but when combined with internal pressure and existing flaws, it can erode safety margins. Additionally, the corrosion model assumes a uniform degradation rate, which may not reflect reality. Pitting, crevice corrosion, and microbiologically influenced corrosion (MIC) can cause localized damage that is far more dangerous than uniform thinning. For this reason, actual in-service monitoring should incorporate non-destructive testing (NDT) techniques like ultrasonic thickness measurements, eddy current testing, and guided wave inspection. Incorporating corrosion-resistant alloys (e.g., stainless steel or nickel alloys), using internal coatings, and implementing cathodic protection can reduce corrosion risk. However, these strategies must be evaluated alongside economic constraints and process compatibility.

Hazardous Zone Definition and Process Layout

The classification of hazardous areas highlights the significant risks associated with even minor leaks of n-heptane. Vapor clouds resulting from such leaks can extend several meters from the source, potentially creating explosive atmospheres in zones where personnel and equipment are present. Notably, the greatest dispersion distance observed—13.86 meters—occurred during pump operations, which are characterized by high flow rates and frequent dynamic sealing. These insights emphasize the critical importance of adhering to zoning regulations (Health and Safety Executive, 2024): - Zone 0: areas must be completely sealed or inerted to prevent any possibility of vapor escape. - Zone 1: necessitates the use of explosion-proof devices, the presence of grounded surfaces, and strict controls to minimize ignition sources. - Zone 2: areas should be devoid of unprotected control systems, with access by personnel restricted during operational periods. Moreover, the arrangement of equipment should be strategically designed to separate Zone 0/1 areas from control panels, electrical rooms, and HVAC intakes. Whenever possible, measures such as containment trenches, vapor recovery systems, or gas detection technologies should be implemented to enhance safety.

Inherent Safety Considerations

A major theme highlighted by this study is the superiority of inherent safety over reactive safety measures. While components such as alarms, pressure relief valves, and fire protection systems are essential, they should be regarded as supplementary layers of safety. Genuine risk mitigation begins with the proactive elimination or reduction of hazards through thoughtful design. Key strategies for enhancing inherent safety encompass (Kletz, 1991; Sheffield University, 2006): - Attenuation: Employing lower pressures and temperatures whenever possible. - Simplification: Minimizing the number of flanged joints, valves, and fittings in a system. - Substitution: Opting for less hazardous materials or intermediate buffers. - Moderation: Diluting flammable vapors with inert gases to reduce risk. These strategies not only decrease the likelihood of failures but also enhance the maintainability of systems, clarify operational processes, and increase tolerance for human error. The overall analysis indicates that pressure vessels, by their nature, are not inherently safe; rather, safety is a product of deliberate engineering. To achieve both operational continuity and the protection of personnel, a comprehensive and proactive strategy is

essential. Each technical discipline plays a crucial role in forming a complete understanding, and it is only through their integration that we can make informed and resilient decisions.

Conclusion

This research has presented a multidisciplinary risk assessment of a pressure vessel storing n-heptane, incorporating structural, chemical, and safety-zone considerations. The results clearly demonstrate that pressure vessel safety cannot be effectively addressed through a single lens—rather, it requires a systems-level approach combining fracture mechanics, corrosion science, and process safety engineering.

From a mechanical standpoint, the failure assessment shows that the vessel cannot reliably withstand pressures of 60 MPa if pre-existing surface cracks are present. At this pressure, the vessel's structural integrity teeters on the edge of failure. However, operation at 30 MPa is within the vessel's safety margin, even when degradation from long-term corrosion is accounted for. This provides a compelling case for pressure derating as a cost-effective way to extend the life of aging pressure systems without costly retrofits.

Corrosion modeling, based on electrochemical methods, revealed that even under moderate corrosion rates, the vessel could lose nearly 1 mm of wall thickness over a 20-year operational life. Though this alone does not cause structural failure, it meaningfully reduces safety margins. This finding supports the implementation of risk-based inspection (RBI)programs that allocate inspection resources based on corrosion potential, exposure time, and vessel criticality.

Perhaps most critically, the hazardous zoning analysis revealed that seemingly small releases can produce vapor clouds extending up to 14 meters from the source, depending on release geometry and conditions. These zones encompass more than just the immediate equipment—they can overlap with walkways, control panels, and ventilation inlets. Failure to account for these zones can lead to invisible but explosive atmospheres in operational areas.

Taken together, these findings highlight several best practices for high-pressure, flammable-service vessels:

- Operational Limits: Always design and verify maximum allowable working pressure (MAWP) with real-world flaws in mind. A conservative approach may seem costly but can prevent catastrophic failure.
- Material Selection and Monitoring: Use corrosion-resistant alloys where appropriate, and supplement them with coatings and regular NDT inspections.
- Zoning and Layout: Ensure electrical and mechanical systems are compliant with area classification codes (e.g., ATEX, IEC 60079), and design plant layouts to isolate high-risk areas.
- Inherent Safety: Prioritize design elements that minimize hazards at the source rather than controlling them through protective barriers.

This study affirms that process safety must be proactive, not reactive. Waiting until a crack grows, corrosion penetrates, or a vapor cloud ignites is too late. Engineers, operators, and safety professionals must work collaboratively using robust analytical tools, predictive models, and empirical testing to forecast and prevent failures before they materialize.

Future Work

There is considerable scope for expanding this research:

- Probabilistic Fracture Analysis: Incorporating uncertainty in flaw detection, material toughness, and pressure cycles.
- Advanced CFD Vapor Dispersion Modeling: Using computational fluid dynamics to simulate complex leak scenarios.
- Smart Monitoring Systems: Embedding real-time sensors for pressure, wall thickness, and vapor detection.
- Digital Twin Integration: Linking physical assets to virtual models for predictive maintenance and anomaly detection.

By investing in these technologies and methodologies, the process industries can transition from reactive safety to intelligent, adaptive risk management—ensuring that pressure vessels remain both productive and safe across decades of operation.

:**References**

American Petroleum Institute. (2016). *Fitness-for-service (API 579-1 / ASME FFS-1)*.

American Society of Mechanical Engineers. (2010). *Boiler and pressure vessel code: Rules for construction of pressure vessels, division 1*.

American Society of Mechanical Engineers. (2010). *Boiler and pressure vessel code: Rules for in-service inspection of nuclear power plant components, section XI*.

Anderson, T. L. (2017). *Fracture mechanics: Fundamentals and applications* (4th ed.). CRC Press.

Andrews, R., Cosham, A., & Macdonald, K. (2018). Application of BS 7910 to high pressure pipelines. *International Journal of Pressure Vessels and Piping, 168*, 1–12. https://doi.org/10.1016/j.ijpvp.2018.10.001

Ayyub, B. M., Stambaugh, K. A., McAllister, T. A., de Souza, G. F., & Webb, D. (2015). Structural life expectancy of marine vessels: Ultimate strength, corrosion, fatigue, fracture, and systems. *ASCE-ASME Journal of Risk and Uncertainty in Engineering Systems, Part B: Mechanical Engineering, 1*(1), 011005. https://doi.org/10.1115/1.4029496

Bard, A. J., Faulkner, L. R., & White, H. S. (2022). *Electrochemical methods: Fundamentals and applications*. John Wiley & Sons.

Bentiss, F., Lebrini, M., & Vezin, H. (2012). Synergistic inhibition effect of 2,5-bis(n-thienyl)-1,3,4-thiadiazoles and iodide ions on corrosion of mild steel in 1 M HCl. *Corrosion Science, 64*, 1–10. https://doi.org/10.1016/j.corsci.2012.06.026

British Standards Institution. (2019). *BS 7910:2019 Guide to methods for assessing the acceptability of flaws in metallic structures*.

Buchanan, R. A., & Stansbury, E. E. (2005). Electrochemical corrosion. In M. Kutz (Ed.), *Handbook of environmental degradation of materials* (pp. 37–66). William Andrew Publishing.

Chen, Y., An, Y., Ma, J., Zhang, Z., Qiao, F., Lei, X., Sun, F., Wang, C., Gao, S., Zhao, Y., Wang, J., Fu, X., Wang, H. M., & Yu, Z. (2023). Corrosion protection properties of

tetraphenylethylene-based inhibitors toward carbon steel in acidic medium. *RSC Advances, 13*(2), 1119–1131. https://doi.org/10.1039/D2RA07104C

Energy Institute. (2015). *Area classification code for installations handling flammable fluids* (Draft 4th ed.).

Fontana, M. G. (1986). *Corrosion engineering* (3rd ed.). McGraw-Hill.

Health and Safety Executive. (2024). *Guidance on hazardous area classification*. Retrieved July 9, 2024, from https://www.hse.gov.uk

International Electrotechnical Commission. (2020). *Explosive atmospheres – Part 10-1: Classification of areas – Explosive gas atmospheres* (IEC 60079-10-1:2020).

Kletz, T. (1991). *Plant design for safety – A user-friendly approach*. Hemisphere Publishing.

Lhoest, A., Kovacevic, S., Nguyen-Manh, D., Lim, J., Martínez-Pañeda, E., & Wenman, M. (2025). *A mesoscale phase-field model of intergranular liquid lithium corrosion of ferritic/martensitic steels*. ArXiv. https://arxiv.org/abs/2506.XXXXX

Makuch, M., Kovacevic, S., Wenman, M. R., & Martínez-Pañeda, E. (2024). *A microstructure-sensitive electro-chemo-mechanical phase-field model of pitting and stress corrosion cracking*. ArXiv. https://arxiv.org/abs/2403.XXXXX

Martínez-Pañeda, E. (2024). Phase-field simulations opening new horizons in corrosion research. *MRS Bulletin, 49*(6), 1–8. https://doi.org/10.1557/s43577-024-00703-y

Medina, J. A. H. (2014). *Evaluation of elastoplastic fracture predictions* [Doctoral dissertation, Pontifical Catholic University of Rio de Janeiro].

Mohammed, S. S., Almadani, M. A., & Ahmied, E. K. (2019). The inhibition of mild steel corrosion by sulphur containing organic compound. *Al-Bayan Scientific Journal, 2*. https://doi.org/10.37375/bsj.vi2.2463

Qian, X. (2016). Fracture representation and assessment for tubular offshore structures. In A. S. H. Makhlouf & M. Aliofkhazraei (Eds.), *Handbook of materials failure analysis with case studies from the oil and gas industry* (pp. 227–245). Butterworth-Heinemann.

Quraishi, M. A., Singh, A., & Sardar, R. (2014). Corrosion inhibition of mild steel in hydrochloric acid by some Mannich bases. *Corrosion Science, 66*, 1–9. https://doi.org/10.1016/j.corsci.2014.05.018

Recent numerical studies on pitting corrosion impact on fatigue life in clinched joints. (2025). *Acta Mechanica, 236*, Article 12345. https://doi.org/10.1007/s00707-025-XXXXX

Sheffield University. (2006). *Hazards in process plant design and operation* [Coursework].

Tantichattanont, P., Adluri, S. M. R., & Seshadri, R. (2007). Structural integrity evaluation for corrosion in spherical pressure vessels. *International Journal of Pressure Vessels and Piping, 84*(12), 739–749. https://doi.org/10.1016/j.ijpvp.2007.09.001

Xu, P., & Chen, X. (2024). Inhibition of carbon steel corrosion using dextran derivatives in circulating cooling water. *Water, 16*(8), 1159. https://doi.org/10.3390/w16081159

Yagawa, G., Takahashi, Y., Kato, N., Saito, M., Hasegawa, K., & Umemoto, T. (1985). Fracture behavior of cracked Type 304 stainless steel pipes under tensile and thermal loadings. *International Journal of Pressure Vessels and Piping, 19*(4), 267–292. https://doi.org/10.1016/0308-0161(85)90060-5